

# Structural and Theoretical Studies of *ortho*-Substituted Triphenylphosphane Ligands and Their Rhodium(I) Complexes

Pekka Suomalainen,<sup>[a]</sup> Sirpa Jääskeläinen,<sup>[a]</sup> Matti Haukka,<sup>[a]</sup> Riitta H. Laitinen,<sup>[b]</sup>  
Jouni Pursiainen,<sup>[b]</sup> and Tapani A. Pakkanen<sup>\*[a]</sup>

**Keywords:** Structure elucidation / P ligands / Rhodium / Molecular modeling

The triarylphosphanes, (*o*-thiomethylphenyl)diphenylphosphane (SP, **1**), (*o*-*N,N'*-dimethylaminophenyl)diphenylphosphane (NP, **2**), and (*o*-methoxyphenyl)diphenylphosphane (OP, **3**) have been structurally characterized. Detailed information on the stereochemistry of the ligands was gathered by spectroscopic (<sup>1</sup>H, <sup>31</sup>P, <sup>13</sup>C NMR) and X-ray crystallographic studies. Molecular modeling methods for investigation of the structures were also applied. It is shown that the geometrical optimization of the ligand can be performed accurately by the ab initio Hartree–Fock method. Further-

more, the steric contribution of the coordinated ligands can be estimated by studying the different conformational states of the free ligands. The coordination abilities of the ligands were studied in reactions with the rhodium compounds Rh<sub>2</sub>(CO)<sub>4</sub>Cl<sub>2</sub> and Rh(NO<sub>3</sub>)<sub>3</sub> under different reaction conditions. The SP and NP ligands yielded mononuclear chelate complexes, while the OP ligand coordinated solely in a monodentate fashion through the phosphorus atom. The crystal structures of the ligands **1–3** and the rhodium(I) complexes [RhCl(CO)(NP)] (**5**) and [RhCl(CO)(OP)<sub>2</sub>] (**6**) are reported.

## Introduction

Increasing research is being done to rationalize the design of homogeneous catalysts for specific industrial applications. The demand for higher selectivity of the several homogenous catalytic reactions has inspired research on the effects of modifying the metal sphere with various ligands. The development of tertiary phosphane ligands began with Wilkinson's catalyst.<sup>[1]</sup> Since then, many sterically and electronically enhanced PX<sub>3</sub> ligands have been investigated, and useful tools have been developed for measuring the properties of these ligands.<sup>[2,3]</sup> Polydentate phosphorus ligands have attracted much interest in the field of homogeneous catalysis. Mixed ligands containing phosphorus together with oxygen, nitrogen or sulfur have been studied in a number of applications including polymerization and oligomerization of olefins,<sup>[4]</sup> carbonylation of methanol,<sup>[5]</sup> and hydroformylation of olefins.<sup>[6]</sup> With the possible hemilabile character of these ligands, a more weakly coordinated donor site may appear between the coordinated/uncoordinated equilibrium, allowing an interesting setup for catalytic reactions. Hemilabile character has earlier been reported for several mixed heteroatom-phosphorus ligands, including ether-phosphanes,<sup>[7]</sup> hydroxyphenyl phosphanes,<sup>[8]</sup> phosphonate-phosphanes,<sup>[9]</sup> and amido-diphosphanes.<sup>[10]</sup> The fluxional behavior of this type of ligand around the metal center is considered to activate CO and H<sub>2</sub> molecules, thus improving the oxo-reactions such as carbonylation and hydroformylation. Recently, Reinius et al. studied the hydro-

formylation of methyl methacrylate (MMA) in the presence of SP, NP, and OP ligands. Exceptional selectivity towards branched methyl- $\alpha$ -formylisobutyrate was found when the SP ligand was used in situ with Rh(NO<sub>3</sub>)<sub>3</sub>.<sup>[11]</sup>

This paper describes structural and complexation studies on three *ortho*-substituted triphenylphosphane derivatives: (*o*-thiomethylphenyl)diphenylphosphane (SP, **1**), (*o*-*N,N'*-dimethylaminophenyl)diphenylphosphane (NP, **2**), and (*o*-methoxyphenyl)diphenylphosphane (OP, **3**). In addition to spectroscopic and crystallographic studies, theoretical investigations of the ligand structures have been carried out to obtain a better understanding of the stereochemistry. We were particularly interested to know whether the steric requirements of the coordinated ligands could be estimated by ab initio calculations of the ligands in the gas phase. The coordination modes of the ligands were studied in reactions with the rhodium compounds Rh<sub>2</sub>(CO)<sub>4</sub>Cl<sub>2</sub> and Rh(NO<sub>3</sub>)<sub>3</sub>. Syntheses at a higher synthesis gas pressure and temperature were carried out to investigate the behavior of the ligands in a catalytic environment.

## Results and Discussion

### Synthesis and Characterization of Substituted Triarylphosphane Ligands

The mono-substituted triphenylphosphane derivatives SP, NP, and OP were prepared according to literature methods.<sup>[11–13]</sup> The X-ray crystal structures of the ligands are reported for the first time. Crystallographic data are given in Table 1. Figure 1 shows an Ortep drawing of the SP ligand. Selected bond parameters for ligands **1–3** are compiled in Table 2. The labeling scheme for the NP and OP ligands is the same as for the SP ligand.

<sup>[a]</sup> Department of Chemistry, University of Joensuu, P. O. Box 111, 80101 Joensuu, Finland  
E-mail: pekka.suomalainen@joensuu.fi

<sup>[b]</sup> Department of Chemistry, University of Oulu, Linnanmaa, 90570 Oulu, Finland

Table 1. Crystallographic data for SP, NP, OP, [Rh(CO)Cl(NP)] (**5**), and [Rh(CO)Cl(OP)<sub>2</sub>] (**6**)

	SP	NP	OP	<b>5</b>	<b>6</b>
Empirical formula	C <sub>19</sub> H <sub>17</sub> PS	C <sub>20</sub> H <sub>20</sub> NP	C <sub>19</sub> H <sub>17</sub> OP	C <sub>21</sub> H <sub>20</sub> CINOPRh	C <sub>39</sub> H <sub>34</sub> ClO <sub>3</sub> P <sub>2</sub> Rh
Mol wt	308.36	305.34	292.30	471.71	750.96
Crystal size, mm	0.3 × 0.2 × 0.2	0.1 × 0.1 × 0.4	0.3 × 0.1 × 0.1	0.3 × 0.2 × 0.1	0.6 × 0.4 × 0.3
Cryst. syst.	Monoclinic	Orthorhombic	Monoclinic	Monoclinic	Monoclinic
Space group	<i>P</i> 2(1)/ <i>c</i>	<i>Pbca</i>	<i>C</i> 2/ <i>c</i>	<i>P</i> 2(1)/ <i>n</i>	<i>P</i> <i>n</i>
$\lambda$ , Å	0.71073	0.71073	0.71073	0.71073	0.71073
<i>a</i> , Å	11.320(2)	16.481(3)	31.324(6)	9.3518(19)	12.826(3)
<i>b</i> , Å	16.151(3)	12.281(2)	7.2730(10)	18.394(4)	10.298(2)
<i>c</i> , Å	9.673(2)	16.932(3)	28.698(6)	11.693(2)	13.296(3)
$\beta$ , deg	109.44(3)	90	90.66(3)	101.74(3)	106.15(3)
<i>V</i> , Å <sup>3</sup>	1667.7(5)	3427.1(10)	6538(2)	1969.3(7)	1686.7(6)
<i>Z</i>	4	8	16	4	2
<i>D</i> <sub>calc</sub> , g/cm <sup>3</sup>	1.228	1.184	1.188	1.591	1.479
$\mu$ mm <sup>-1</sup>	0.281	0.157	0.164	1.094	0.718
<i>T</i> , °C	293(2)	293(2)	293(2)	120(2)	120(2)
$\theta$ range, deg	3.16 to 26.48	2.98 to 25.00	2.88 to 25.00	2.84 to 27.48	1.98 to 27.47
No. of unique rflns	3405	2991	5289	4446	7493
No. of obsd. data <sup>[a]</sup>	2755	1359	2289	3939	7268
No. of params	242	200	380	315	419
<i>R</i> <sub>1</sub>	0.0380	0.0605	0.0713	0.0231	0.0241
<i>wR</i> <sub>2</sub>	0.0987	0.0907	0.1683	0.0549	0.0557
Largest diff. Peak and hole, e Å <sup>-3</sup>	0.154 −0.186	0.228 −0.208	0.702 −0.215	0.421 −0.875	0.588 −0.516

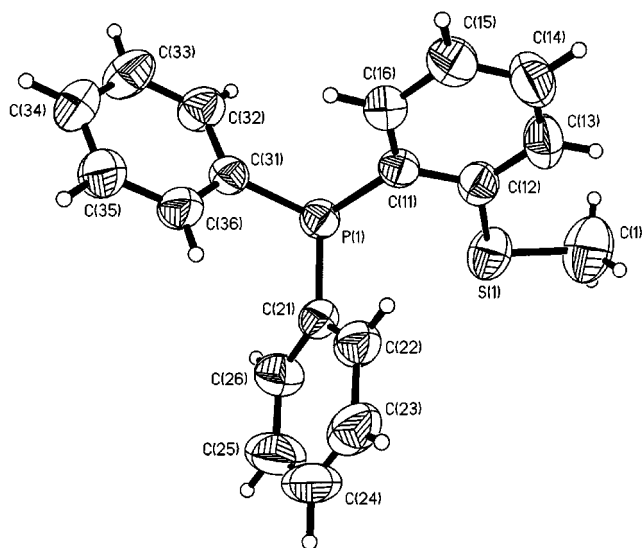
[a] *I* > 2 $\sigma$ .

Figure 1. Ortep drawing of the SP ligand with thermal ellipsoids at 50% level

Table 2. Selected bond lengths, angles, and torsional angles for the SP, NP, and OP ligands

Atoms <sup>[a]</sup>	SP (1)	NP (2)	OP (3)
Bond lengths (Å)			
P(1)–C(11)	1.833 (2)	1.828 (3)	1.830 (5)
P(1)–C(21)	1.830 (2)	1.831 (3)	1.838 (5)
P(1)–C(31)	1.829 (2)	1.824 (3)	1.828 (5)
X(1)–C(1)	1.783 (3)	1.467 (4)	1.429 (6)
X(1)–C(2)	–	1.462 (4)	–
C(12)–X(1)	1.767 (2)	1.439 (4)	1.375 (6)
P(1A)–C(11A)	–	–	1.838 (5)
P(1A)–C(21A)	–	–	1.839 (5)
P(1A)–C(31A)	–	–	1.818 (5)
Bond angles (deg)			
C(31)–P(1)–C(21)	101.8 (7)	101.1 (2)	102.1 (2)
C(31)–P(1)–C(11)	102.8 (7)	102.0 (2)	100.9 (2)
C(21)–P(1)–C(11)	102.1 (7)	101.5 (2)	100.9 (2)
C(12)–X(1)–C(1)	103.1 (1)	112.0 (3)	118.7 (5)
C(12)–X(1)–C(2)	–	113.5 (3)	–
C(12A)–O(1A)–C(1A)	–	–	121.4 (7)

[a] X = S, N or O.

Table 3. Low lying conformations and corresponding cone angles of ligands

Conformation	$\Delta E$ (kJ/mol)/ $\Theta$ (deg)					
	SP		OP		NP	
Conf 1*	0	158	0	166	0	180
Conf 2	2.55	158	8.94	156	27.40	153
Conf 3	23.78	155	12.61	153		
Conf 4	32.13	153				

\* Global minimum.

### Conformational Flexibility of the Ligands

The equilibrium geometries of the SP, OP, and NP ligands were first determined by optimizing the structures with the ab initio Hartree–Fock method using a 3–21G\* basis set. Starting from the initial geometries, a conformational analysis was carried out by rotating the torsional angles of the three phenyl rings. Several local minima were identified and subsequently optimized with the HF/3–21G\* method. The energies of the minima relative to the ground state are shown in Table 3.

The steric crowding of the free ligands was measured using Tolman's semi-cone angle concept.<sup>[2]</sup> The cone angles of the free ligands were calculated for the ground states and

for low lying conformations. As shown in Table 3, the cone angles are widest for the ground states and narrow for the higher energy conformers, giving an indication of the en-

ergy demands of the steric repulsion. In the lowest energy conformations, the maximum semi-cone angles are always determined by the *m*-hydrogen atoms of the phenyl rings and by one of the hydrogen atoms in the  $-XCH_3$  group. In this manner, the ligands can be arranged in decreasing order of bulkiness:  $SP = OP < NP$ . For the higher energy conformations of the ligands, the cone angles diminish because the substituted phenyl ring(s) rotates in such a way that the  $-XCH_3$  group becomes located inside the cone and no longer directly affects the maximum semi-cone angle. This eventually leads to identical values of cone angles.

### Synthesis and Characterization of Rhodium Phosphane Complexes

Two different rhodium sources,  $Rh_2(CO)_4Cl_2$  and  $Rh(NO_3)_3$ , were used to prepare the complexes. Variations in atmosphere, temperature, pressure, and solvent, were introduced to clarify the various possibilities for the reaction pathways, and to proceed step-by-step from milder reaction conditions to a more severe, actual catalytic environment. At room temperature, the syntheses were carried out in an atmosphere of either nitrogen or carbon monoxide. Conditions nearer to a catalytic environment were obtained when the reactions were carried out in autoclaves that were heated to 100 °C and pressurized to 20 bar with carbon monoxide or synthesis gas ( $CO/H_2$ ). The reaction time in the pressurized synthesis reactions was 4 h, after which the autoclaves were allowed to cool to room temperature.

### Reactions With the SP Ligand

A yellow precipitate was isolated after  $Rh_2(CO)_4Cl_2$  and the SP ligand were allowed to react in a methanol solution at room temperature and under an atmosphere of nitrogen. The product was identified crystallographically as the square-planar rhodium compound  $[Rh(CO)Cl(SP)]$  (**4**) with the SP ligand chelating through the sulfur and phosphorus atoms. The IR spectrum of **4** shows a CO stretching vibration at  $2010\text{ cm}^{-1}$ , while the  $^{31}P$  NMR spectrum gives a doublet at  $\delta = 67.2$  with  $J_{Rh-P} = 152\text{ Hz}$ . Dilworth et al.<sup>[14]</sup> have previously reported the synthesis of a brown precipitate, which they proposed on the basis of spectroscopic investigation to be compound **4**. More recently, Steeg et al.<sup>[15]</sup> published a crystallographic characterization of the same compound, which was, however, reached by a different route.

Compound **4** was again formed under an atmosphere of carbon monoxide in toluene solution. Likewise the formation of **4** was observed under syngas pressure ( $CO/H_2$  20bar) and at high temperature (100 °C), but another doublet in the  $^{31}P$  NMR spectrum was found at  $\delta = 48.9$  with a smaller coupling constant of 77 Hz. This new signal was assigned to an isomeric form of complex **4** with the carbonyl group *trans* to phosphorus, since such coordination gives a lower shift and coupling constant than the corresponding orientation with phosphorus *trans* to chloride.<sup>[16]</sup>

The reaction between  $Rh(NO_3)_3 \cdot 2H_2O$  and SP in a catalytic environment gave peaks at  $2034$  and  $1873\text{ cm}^{-1}$  in the IR spectrum, as well as a broad line at  $\delta = 28$  in the  $^{31}P$

NMR spectrum. Resemblance of the spectroscopic data to those of the rhodium diphosphane compounds  $HRh(CO)_x(P)_y$  prepared under similar reaction conditions can be seen.<sup>[17]</sup> In addition, the fluctuation of the SP coordination is possible. Furthermore, the formation of polynuclear carbonyl compounds is possible as a result of degradation of the ligand under severe reaction conditions.<sup>[18]</sup>

### Reactions With the NP Ligand

Methanol solutions of  $Rh_2(CO)_4Cl_2$  and NP were mixed at room temperature under an atmosphere of nitrogen to form a yellow precipitate. The product was identified crystallographically as the monometallic chelate species,  $[Rh(CO)Cl(NP)]$  (**5**), bonded through nitrogen and phosphorus (Figure 2). The structure shows a planar geometry around the rhodium atom with a slight deviation from ideal. The largest discrepancy is along the axis  $P(1)-Rh(1)-Cl(1)$  where the angle is  $174.7(2)^\circ$ . A shorter  $Rh-C(4)$  distance than in complex **4** indicates the stronger

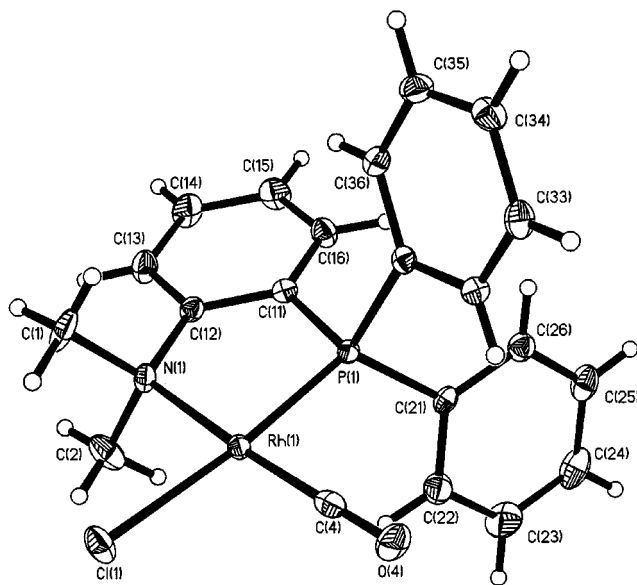


Figure 2. Ortep drawing of  $Rh(CO)ClNP$  with thermal ellipsoids at 50% level

Table 4. Selected bond angles and distances for  $Rh(CO)Cl(NP)$  (**5**)

Atoms	Bond lengths (Å)
$Rh(1)-P(1)$	2.3308(10)
$Rh(1)-P(2)$	2.3335(10)
$Rh(1)-Cl(1)$	2.4131(10)
$Rh(1)-C(4)$	1.827(5)
$C(4)-O(4)$	0.989(5)
Atoms	Bond angles (deg)
$C(4)-Rh(1)-P(1)$	87.26(10)
$C(4)-Rh(1)-P(2)$	92.21(9)
$P(1)-Rh(1)-P(2)$	179.39(4)
$C(4)-Rh(1)-Cl(1)$	178.40(11)
$P(1)-Rh(1)-Cl(1)$	92.89(3)
$P(2)-Rh(1)-Cl(1)$	87.63(3)

electron-donor character of the NP ligand. The flow of electron density to the rhodium increases  $\pi$ -back donation to the carbonyl. This is further observed in the CO stretching frequencies of  $2010\text{ cm}^{-1}$  and  $1995\text{ cm}^{-1}$  for **4** and **5**, respectively. The  $^{31}\text{P}$  spectrum of **5** shows a doublet at  $\delta = 56.8$  with a Rh–P coupling of 171 Hz.

When the same reactants were allowed to react in the autoclave (toluene,  $100\text{ }^{\circ}\text{C}$ , 20 bar CO, 4 hours), species **5** was again isolated and characterized by its IR stretching vibration and elemental analysis. The same product was observed when a CO/ $\text{H}_2$  atmosphere was applied to the reaction. An IR absorption at  $1995\text{ cm}^{-1}$  was found, but also an additional peak at  $2071\text{ cm}^{-1}$  appeared in the spectrum, suggesting the formation of a  $\text{Rh}_6(\text{CO})_{16}$  cluster. The synthesis and stereochemistry of **5** has previously been discussed by Roundhill et al.<sup>[19,20]</sup>

The strong chelating ability of the NP ligand was also observed in the reaction with  $\text{Rh}(\text{NO}_3)_3 \cdot 2\text{H}_2\text{O}$  at room temperature under a CO atmosphere. From the assignment of a doublet at  $\delta = 57.9$  (141 Hz) in the  $^{31}\text{P}$  NMR spectrum and an IR absorption at  $1995\text{ cm}^{-1}$ , we deduced that a chelate compound was formed with the NP ligand. Under more severe reaction conditions, the product from the reaction with  $\text{Rh}(\text{NO}_3)_3 \cdot 2\text{H}_2\text{O}$  and NP afforded similar spectroscopic data to those obtained with the SP ligand, suggesting corresponding species.

### Reactions With the OP Ligand

$\text{Rh}_2(\text{CO})_4\text{Cl}_2$  and the OP ligand were allowed to react under nitrogen at room temperature in a methanol solution to form a yellow precipitate. The compound, *trans*- $[\text{Rh}(\text{CO})\text{Cl}(\text{OP})_2]$  (**6**), was characterized crystallographically as a tetracoordinate monocarbonyl complex with two phosphorus ligands bonded in a monodentate fashion (Fig-

ure 3). Analogous  $[\text{RhX}(\text{CO})(\text{PAr}_3)_2]$  ( $\text{X} = \text{Cl}, \text{I}, \text{Br}$ ) structures have been reported previously.<sup>[21–23]</sup> Compound **6** gives a strong CO stretching vibration at  $1974\text{ cm}^{-1}$  and the  $^{31}\text{P}$  NMR spectrum shows a doublet at  $\delta = 23.2$  with a Rh–P coupling constant of 129 Hz. The crystallographic data for **6** are given in Table 1. Selected bond lengths and angles are given in Table 5. Under similar reaction conditions in dichloromethane, the reaction proceeds differently, resulting in strong IR absorptions at 2090 and  $2010\text{ cm}^{-1}$ , characteristic of either monometallic *cis*-dicarbonyl or dimeric, doubly five-coordinated phosphane derivatives.<sup>[24]</sup> At an elevated pressure and temperature, complex **6** was again the main product.

Table 5. Selected bond angles and distances for  $\text{Rh}(\text{CO})\text{Cl}(\text{OP})_2$  (**6**)

Atoms	Bond lengths (Å)
Rh(1)–C(4)	1.807(2)
Rh(1)–P(1)	2.1947(6)
Rh(1)–N(1)	2.1865(2)
Rh(1)–Cl(1)	2.3867(7)
C(4)–O(4)	1.150(2)
P(1)–C(21)	1.824(2)
P(1)–C(31)	1.8216(2)
P(1)–C(11)	1.815(2)
N(1)–C(12)	1.477(2)
N(1)–C(1)	1.496(3)
N(1)–C(2)	1.487(3)
Atoms	Bond angles (deg)
C(4)–Rh(1)–P(1)	91.24(7)
C(4)–Rh(1)–N(1)	176.26(7)
P(1)–Rh(1)–N(1)	85.03(5)
C(4)–Rh(1)–Cl(1)	92.62(7)
P(1)–Rh(1)–Cl(1)	174.696(2)
X(1)–Rh(1)–Cl(1)	91.11(5)
O(4)–C(4)–Rh(1)	178.94(2)

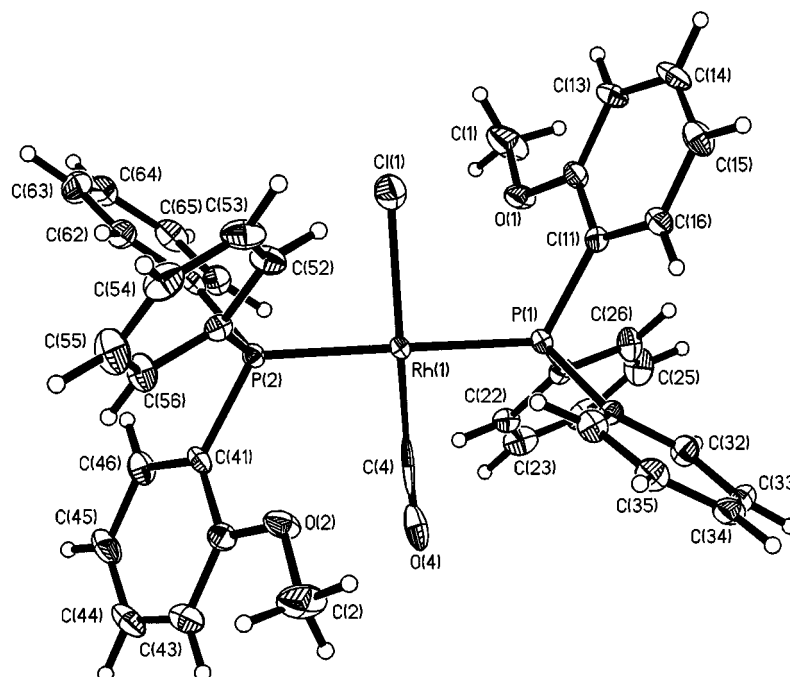


Figure 3. Ortep drawing of  $\text{Rh}(\text{CO})\text{Cl}(\text{OP})_2$  with thermal ellipsoids at 50% level



The reaction between  $\text{Rh}(\text{NO}_3)_3 \cdot 2\text{H}_2\text{O}$  and the OP ligand in a methanol solution under an atmosphere of CO resulted in a greenish-yellow solid. This compound gives a strong IR absorbance at  $1974\text{ cm}^{-1}$ , indicating a geometry similar to that of complex **6**. Crystallization from dichloromethane led to a mixture of yellow and green crystals. The yellow crystals turned out to be species **6**, evidently formed through exchange of an  $\text{NO}_3$  group for the chlorine atom. The green crystals have a linear  $\text{P}-\text{Rh}-\text{P}$  skeleton, as in complex **6**, with a bidentate  $\text{NO}_3$  ligand attached by two oxygen atoms. However, the remaining ligands were disordered, and crystallization of two different species also seemed probable. In the  $^{31}\text{P}$  NMR spectrum, the green crystals give rise to a doublet at  $\delta = 20.2$  with  $J_{\text{Rh}-\text{P}} = 153\text{ Hz}$ .

The presence of **6** was again observed at elevated temperature and 20 bar syngas pressure. Additional absorptions were detected at  $2034$  and  $1873\text{ cm}^{-1}$  in the IR spectrum, and there is a broad line at  $\delta = 28$  in the  $^{31}\text{P}$  NMR spectrum. Similar species as observed with the SP and NP ligands are proposed.

No evidence was found for the chelating character of the OP ligand. The monodentate binding mode of the OP ligand has also been observed by Trzeciak et.al.<sup>[8]</sup> However, they found that substitution of a methoxy group for a hydroxyl group changes the reactivity of the ligand, resulting in stable chelate complexes.

### Comparison Between Solid State and Calculated Structures

Reliable predictions of ligand geometries were obtained using the Hartree–Fock method. The geometries of the ground-state structures and the X-ray structures of the ligands deviate by only a few hundredths of an angstrom in bond lengths and one degree in bond angles. The cone angle values based on the solid state structures of the free ligands fall within the cone angle range measured for the different gas-phase conformers. Only the SP ligand was found to have a greater angle in the solid state. The cone angle data for the ligands are shown in Table 6. A closer investigation of the coordinated OP ligand in complex **6** revealed a similar geometry to its lowest energy conformation. Being in the *trans* position to each other, the two OP ligands can lie near the low energy conformation. We can assume that the phosphane does not encounter a significant amount of steric interaction from the CO or Cl ligands. A comparison of the structures of the free and bonded OP ligand is shown in Figure 4. The presence of a bidentate coordination mode in compounds **4** and **5** makes a similar examination of these compounds more difficult.

Table 6. Cone angle values based on different structural data

Ligand	Free ligand (X-ray)	Flexibility range (HF 3–21G*)	Coordinated ligands (X-ray) $\text{Rh}(\text{CO})\text{Cl}(\text{L})_2$ ( <b>6</b> )
SP	164	153–158	-
NP	176	153–180	-
OP	162	153–166	154, 155

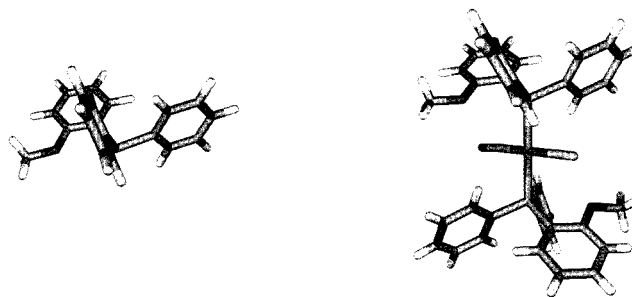


Figure 4. Comparison of the lowest energy conformations of (*o*-methoxyphenyl)diphenylphosphane and the coordinated ligand

### Conclusion

Through a detailed examination of the conformational variations of the free ligand structures in the gas phase, we were able to estimate the steric requirements of the solid-state structures of the free and coordinated ligands. However, the multiple binding sites of the ligands may lead to highly strained conformations, which are hard to predict on the basis of the free ligand structures.

The coordination preference of the ligand in the prepared rhodium complexes was influenced by the type of donor atom in the *ortho* position of the phenyl ring. The strong  $\sigma$ -donor ligands, SP and NP, both yielded chelate species independently of the reaction conditions. In contrast, the OP ligand was found to coordinate in a monodentate fashion.

### Experimental Section

**General:** All the syntheses were carried out using standard Schlenk techniques under an atmosphere of nitrogen. Other gases, carbon monoxide and synthesis gas ( $\text{CO}/\text{H}_2$ ), were of high purity grade (99.997%) and were purchased from AGA and MG, respectively. The solvents, methanol and toluene (p.a. grade), were deoxygenated with nitrogen prior to use.  $\text{Rh}_2(\text{CO})_4\text{Cl}_2$  was prepared according to a literature method<sup>[25]</sup> and  $\text{Rh}(\text{NO}_3)_3 \cdot 2\text{H}_2\text{O}$  was purchased from Alfa. NMR spectra were recorded on a Bruker AM250 spectrometer.  $^{31}\text{P}$  spectra were referenced to 85%  $\text{H}_3\text{PO}_4$ . Elemental analyses were done with a Perkin–Elmer 2400 Series II CHNS/O analyzer. High-pressure synthesis reactions were conducted in 100 mL Berghof autoclaves with a 60 mL Teflon liner. In a typical run, the autoclave was charged in a glovebox with the rhodium compound, ligand, and solvent (toluene). The autoclaves were then sealed and pressurized with either  $\text{H}_2/\text{CO}$  (1:1) or CO to 20 bar. The autoclaves were heated to  $100\text{ }^\circ\text{C}$ , with the temperature controlled and monitored by an internal thermocouple. After four hours reaction time, the autoclaves were cooled slowly and brought to normal atmospheric pressure. The Gaussian 94<sup>[26]</sup> and Sybyl<sup>[27]</sup> programs were used in modeling. The 3–21G\* basis set was used for geometric optimizations at the Hartree–Fock level. In the conformational analyses, the single point energies were calculated with the grid-search method of Sybyl, and the final geometries were determined with the HF/3–21G\* method. The phenyl rings were rotated  $180^\circ$  and the substituted phenyl ring was rotated  $360^\circ$  in increments of  $20^\circ$ . For cone angle determinations, the metal–phosphorus distance was fixed at  $2.28\text{ \AA}$ . A dummy atom was used for free ligands.

**Rh(CO)ClSP (4):** Rh<sub>2</sub>(CO)<sub>4</sub>Cl<sub>2</sub> (25 mg, 0.064 mol) and SP (40 mg, 0.129 mol) were dissolved in methanol in separate flasks. The ligand solution was added dropwise to the solution of the rhodium compound. The yellow precipitate that formed was filtered, washed with methanol, and quickly dried under vacuum. Yellow crystals for X-ray studies were crystallized from CH<sub>2</sub>Cl<sub>2</sub>. — C<sub>20</sub>H<sub>17</sub>ClPRhS (474.73): calcd. C 50.60, H 3.61, S 6.75; found C 50.67, H 3.62, S 6.89. — IR (CH<sub>2</sub>Cl<sub>2</sub>): ν(CO) = 2010 cm<sup>-1</sup>. — <sup>31</sup>P NMR: δ = 67.5 [d, J(Rh–P) = 152 Hz].

**Rh(CO)ClNP (5):** Rh<sub>2</sub>(CO)<sub>4</sub>Cl<sub>2</sub> (100 mg, 0.257 mol) and NP (80 mg, 0.262 mol) were dissolved in methanol in separate Schlenk flasks. The ligand solution was added dropwise to the solution of the rhodium compound. Rapid formation of a yellow precipitate was observed and the reaction was allowed to continue for 2 hours. The precipitate was filtered, washed with methanol and dried under vacuum. Yellow crystals for X-ray studies were obtained from a CH<sub>2</sub>Cl<sub>2</sub>/hexane solution. — C<sub>21</sub>H<sub>20</sub>ClPRhS: calcd. C 53.47, H 4.27, N 2.97; found C 53.27, H 4.31, N 3.14. — IR (CH<sub>2</sub>Cl<sub>2</sub>): ν(CO) = 1995 cm<sup>-1</sup>. — <sup>31</sup>P NMR: δ = 56.8 [d, J(Rh–P) = 171 Hz].

**Rh(CO)Cl(OP)<sub>2</sub> (6). Method 1:** Rh<sub>2</sub>(CO)<sub>4</sub>Cl<sub>2</sub> (100 mg, 0.257 mol) and OP (150 mg, 0.3763 mol) were dissolved in methanol in separate flasks. The ligand solution was added dropwise to the precursor solution. The yellow precipitate that formed was filtered, washed with methanol, and quickly dried under vacuum. Yellow crystals for X-ray studies were crystallized from a CH<sub>2</sub>Cl<sub>2</sub>/hexane solution. — C<sub>39</sub>H<sub>34</sub>ClO<sub>3</sub>P<sub>2</sub>Rh: calcd. C 62.37, H 4.56; found C 62.07, H 4.54. — IR (CH<sub>2</sub>Cl<sub>2</sub>): ν(CO) = 1974 cm<sup>-1</sup>. — <sup>31</sup>P NMR: δ = 23.5 [d, J(Rh–P) = 130 Hz].

**Method 2:** Rh<sub>2</sub>(CO)<sub>4</sub>Cl<sub>2</sub> (25 mg, 0.064 mol) and OP (55 mg, 0.3763 mol) were packed into the autoclave together with 5 mL of toluene. The autoclave was pressurized to 20 bar (CO/H<sub>2</sub>) and heated to 100 °C. After four hours the autoclave was cooled and brought to normal atmospheric pressure. The yellow precipitate that formed was filtered, washed with toluene, and dried under vacuum.

**X-ray Crystallographic Study:** X-ray diffraction data were collected with a Nonius KappaCCD diffractometer using Mo-K<sub>α</sub> radiation (λ = 0.71073 Å) and φ-scan or combined φ/ω-scan data collection mode with a Collect<sup>[28]</sup> data collection program. The Denzo and Scalepack<sup>[29]</sup> programs were used for cell refinements and data reduction. All structures were solved by direct methods using the SHELXS97<sup>[30]</sup> program with the WinGX<sup>[31]</sup> graphical user interface or by using the SHELXTL v5.1<sup>[32]</sup> program package. The structure refinements were carried out with SHELXL97.<sup>[33]</sup> For compounds OP, NP, Rh(CO)Cl(SP), and Rh(CO)Cl(OP)<sub>2</sub>, hydrogen atoms were constrained to ride on their parent atom. [aromatic hydrogens: C–H = 0.93 Å, U<sub>iso</sub> = 1.2(C<sub>eq</sub>) at 293 K and C–H = 0.95 Å, U<sub>iso</sub> = 1.2(C<sub>eq</sub>) at 120 K; methyl hydrogens: C–H = 0.96 Å, U<sub>iso</sub> = 1.5(C<sub>eq</sub>) at 293 K and C–H = 0.95 Å, U<sub>iso</sub> = 1.2(C<sub>eq</sub>) at 120 K]. For compound 5 and SP, all atoms were located from the difference Fourier map. In the former case, the hydrogen atoms were refined isotropically, and in the latter case with constant U<sub>iso</sub> = 0.08. The structure of [Rh(CO)Cl(OP)<sub>2</sub>] (6) was solved as a racemic twin (Flack parameter 0.48952) in the acentric space group *Pn*.

Crystallographic data are summarized in Table 1 and selected bond lengths and angles for the ligands are presented in Table 2, Table 4 and Table 5.

Crystallographic data (excluding structure factors) for the structure(s) reported in this paper have been deposited with the Cambridge Crystallographic Data Centre as supplementary publication no. CCDC-140374 (3), -140375 (1), -140376 (2), -140377

(6), -140378 (5). Copies of the data can be obtained free of charge on application to CCDC, 12 Union Road, Cambridge CB2 1EZ, UK [Fax: (internat.) + 44–1223/336–033; E-mail: deposit@ccdc.cam.ac.uk].

- [1] D. Evans, J. A. Osborn, G. Wilkinson, *J. Chem. Soc.* **1968** 3133.
- [2] C. A. Tolman, *Chem. Rev.* **1977**, 77, 313.
- [3] C. P. Casey, G. T. Whiteker, *Isr. J. Chem.* **1990**, 30, 299.
- [4] G. Braca, A. M. Raspolli Galletti, M. Di Girolamo, G. Sbrana, R. Silla, P. Ferrarini, *J. Mol. Cat.* **1995**, 96, 203.
- [5] A. Bader, E. Lindner, *Coord. Chem. Rev.* **1991**, 108, 27.
- [6] C. Abu-Gnim, I. Amer, *J. Mol. Cat.* **1993**, 85, L275.
- [7] E. Lindner, K. Gierling, B. Keppeler, H. A. Mayer, *Organometallics* **1997**, 16, 3531.
- [8] A. M. Trzeciak, J. J. Ziolkowski, T. Lis, R. Choukroun, *J. Organomet. Chem.* **1999**, 575, 87.
- [9] S. Bischoff, A. Weight, H. Miessner, B. Lucke, *Energy & Fuels* **1996**, 10, 520.
- [10] K. K. Hii, M. Thornton-Pett, A. Jutand, R. P. Tooze, *Organometallics* **1999**, 18, 1887.
- [11] H. K. Reinius, R. H. Laitinen, A. O. I. Krause, J. T. Pursiainen, *Catal. Lett.* **1999**, 60, 65.
- [12] D. W. Meek, G. Dyer, M. O. Workman, *Inorganic Syntheses* **1976**, 16, 168.
- [13] E. Meintjies, E. Singleton, R. Schmutzler, M. Sell, *S. Afr. J. Chem.* **1985**, 38, 115.
- [14] J. R. Dilworth, J. R. Miller, N. Wheatley, M. J. Baker, J. G. Sunley, *J. Chem. Soc., Chem. Commun.* **1995**, 1579.
- [15] N. Steeg, R. Kramolowsky, *Z. Kristallogr.* **1997**, 212, 273.
- [16] J. F. Nixon and A. Pidcock, *Phosphorus-31 NMR Spectra of Coordination Compounds*, *Annu. Rev. NMR Spectrosc.*, **1969**, 2, 345.
- [17] A. Castellanos-Paez, S. Castillion, C. Claver, *Organometallics* **1998**, 17, 2543.
- [18] G. J. H. Buisman, E. J. Vos, P. C. J. Kamer, P. W. N. M. van Leeuwen, *J. Chem. Soc., Dalton Trans.* **1995**, 409.
- [19] D. M. Roundhill, R. A. Bechtold, S. G. N. Roundhill, *Inorg. Chem.* **1980**, 19, 284.
- [20] T. B. Rauchfuss, D. M. Roundhill, *J. Am. Chem. Soc.* **1973**, 3098.
- [21] A. Ceriotti, G. Ciani, A. Sironi, *J. Organomet. Chem.* **1983**, 247, 345.
- [22] F. R. Hartley, S. G. Murray, D. M. Potter, *J. Organomet. Chem.* **1983**, 254, 119.
- [23] R. H. Laitinen, J. Soininen, P. Suomalainen, T. A. Pakkanen, M. Ahlgren, J. Pursiainen, *Acta Chem. Scand.* **1999**, 53, 53.
- [24] [24a] R. Poilblanc, *J. Organomet. Chem.* **1975**, 94, 241. — [24b] P. Uguagliati, G. Deganello, U. Belluco, *Inorg. Chim. Acta* **1974**, 9, 203. — [24c] R. Poilblanc, J. Gallay, *J. Organomet. Chem.* **1971**, 27, C53.
- [25] J. A. Cleverty, G. Wilkinson, *Inorganic Syntheses*, Vol. 8, McGraw-Hill, New-York, **1966**, p.211
- [26] M. J. Frisch, G. W. Trucks, H. B. Schlegel, P. M. W. Gill, B. G. Johnson, M. A. Robb, J. R. Cheeseman, T. Keith, G. A. Petersson, J. A. Montgomery, K. Raghavachari, M. A. Al-Lahman, V. G. Zakrzewski, J. V. Ortiz, J. B. Foresman, J. Cioslowski, B. B. Stefanov, A. Nanayakkara, M. Challacombe, C. Y. Peng, P. Y. Ayala, W. Chen, M. W. Wong, J. L. Andres, E. S. Replogle, R. Gomperts, R. L. Martin, D. J. Fox, J. S. Binkley, D. J. Defrees, J. Baker, J. P. Stewart, M. Head-Gordon, C. Gonzales, J. A. Pople, Gaussian, Inc., Pittsburgh PA, 1995
- [27] Sybyl 6.03; Tripos Associates, 1699 S. Hanley Road, Suite 303, St. Louis, MO 63144.
- [28] Collect: Data Collection Software, Enraf–Nonius, Delft, The Netherlands, **1999**.
- [29] Z. Otwinowski, W. Minor, *Processing of X-ray Diffraction Data Collected in Oscillation Mode, Methods in Enzymology, Volume 276, Macromolecular Crystallography, Part A*, C. W. Carter, Jr. and R. M. Sweet, Eds., Academic Press, **1997**, p. 307–326.
- [30] G. M. Sheldrick, SHELXS97, Program for Crystal Structure Determination, University of Göttingen, Germany, **1997**.

- <sup>[31]</sup> L. J. Farrugia, WinGX v1.61 – A Windows Program for Crystal Structure Analysis, University of Glasgow, Glasgow, **1998**.
- <sup>[32]</sup> G. M. Sheldrick, SHELXTL Version 5.1, Bruker Analytical X-ray Systems, Bruker AXS, Inc. Madison, Wisconsin, USA, **1998**.
- <sup>[33]</sup> G. M. Sheldrick, SHELXL97, Program for Crystal Structure Refinement, University of Göttingen, Germany, **1997**.

Received February 15, 2000  
[I00242]